ARTICLE IN PRESS
Alexandria Engineering Journal (2022) xxx, xxx–xxx

HOSTED BY
ELSEVIER

Alexandria University
Alexandria Engineering Journal
www.elsevier.com/locate/aej
www.sciencedirect.com

ORIGINAL ARTICLE

# Heat absorption/generation effect on MHD heat transfer fluid flow along a stretching cylinder with a porous medium

Y. Dharmendar Reddy [a], B. Shankar Goud [b,*], Kottakkaran Sooppy Nisar [c], B. Alshahrani [d], Mona Mahmoud [d], Choonkil Park [e,*]

[a] Department of Mathematics, Anurag University, Hyderabad, Telangana State 500088, India
[b] Department of Mathematics, JNTUH University College of Engineering, Hyderabad, Telangana State 500085, India
[c] Department of Mathematics, College of Arts and Science, Wadi Aldawaser, 11991, Prince Sattam bin Abdulaziz University, Saudi Arabia
[d] Department of Physics, College of Science, King Khalid University, P.O. Box 9004, Abha 61413, Saudi Arabia
[e] Research Institute for Natural Sciences, Hanyang University, Seoul 04763, Republic of Korea

Received 14 July 2022; revised 25 August 2022; accepted 28 August 2022

KEYWORDS

MHD;
Stretching cylinder;
Heat source/sink;
Heat Transfer;
Porous medium

**Abstract** The current study reveals the impact of MHD heat transfer properties of an incompressible viscous fluid were numerically solved across a continuously expanding horizontal cylinder immersed in a porous material in the existence of internal heat production/sink. The partial differential equations which govern the fluid flow with boundary constraints were converted to a collection of non-linear ODE's with the aid of similarity variables and then numerically solved by using Keller-Box approach. The components of fluid velocity, temperature, as well as friction factor, and rate of heat transfer were all calculated numerically. Graphs and tables illustrate the fluid velocity and heat transfer properties for several Prandtl numbers, and magnetic parameters. The main goal of the current findings is to examine how the magnetic field $M$, $Pr$, and the heat absorption/generation factor $Q$ influence the velocity and temperature gradients along a stretching cylinder. It is projected that the rise in the curvature parameter and the porosity factor would contribute to the enhancement of the temperature gradient in the boundary layer area around the cylinder.



## 1. Introduction

Heat transfer induced by mixed and natural convection in a fluid porous saturated medium has been studied in a broad range of technical applications, including petroleum industries, plasma research, MHD power generators, geothermal systems,

* Corresponding authors.
E-mail addresses: dharmayanala@gmail.com (Y. Dharmendar Reddy), bsgoud.mtech@gmail.com (B. Shankar Goud), ksnisar1@gmail.com (K.S. Nisar), bserhany@kku.edu.sa (B. Alshahrani), mona17477@yahoo.com (M. Mahmoud), baak@hanyang.ac.kr (C. Park).
Peer review under responsibility of Faculty of Engineering, Alexandria University.

https://doi.org/10.1016/j.aej.2022.08.049
1110-0168 

**Nomenclature**

| | |
|---|---|
| $u$ | component of velocity along $x$-direction (m/s) |
| $T$ | fluid temperature inside the thermal boundary layer (K) |
| $\sigma$ | electrical conductivity $\left(\Omega^{-1}\mathrm{m}^{-1}\right)$ |
| $v$ | component of velocity along $r$-direction (m/s) |
| $M = \frac{\sigma B^2 l}{\rho U}$ | magnetic parameter |
| $Q_0$ | volumetric rate of heat source/sink $\left(\mathrm{Kg\,m^{-1}}\right)$ |
| $\alpha$ | thermal diffusivity $(\mathrm{m^2\,s^{-1}})$ |
| $Pr = \frac{v}{\alpha}$ | Prandtl number |
| $K_p$ | porous medium permeability |
| $l$ | characteristic length |
| $T_\infty$ | temperature in the free stream (K) |
| $v$ | kinematic viscosity $(\mathrm{m^2\,s^{-1}})$ |
| $T_0$ | reference temperature of the fluid |
| $Q = \frac{Q_0 l}{U\rho C_p}$ | heat generation/absorption parameter |
| $\rho$ | fluid density $(\mathrm{kg\,m^{-3}})$ |
| $C_p$ | specific heat at constant pressure $(\mathrm{J\ kg^{-1}\ K^{-1}})$ |
| $U$ | reference velocity |
| $\psi$ | stream function $(\mathrm{m^2\ s^{-1}})$ |
| $\beta = \left(\frac{vl}{a^2 U}\right)^{1/2}$ | curvature parameter |
| $K = \frac{vl}{UK_p}$ | permeability parameter |
| $n$ | surface temperature exponent. |
| $\kappa$ | fluid thermal conductivity $\left(\mathrm{kg\ m\,s^{-3}\ K^{-1}}\right)$ |
| $\mu$ | fluid viscosity $(\mathrm{kg\ m^{-1}\ s^{-1}})$ |

insulation of heat, drying technologies, catalytic reactors, food business, and the solar energy collectors. Heat transfer around cylinders has recently gained popularity owing to its numerous practical uses in electronics chilling, design of thermal buildings, drilling processes, energy generation in geothermal, marketable refrigeration, and manufacturing of float glass. Numerous investigations have focused on hydrodynamic flow and heat transmission across stretched cylinders and flat plates as a result of their widespread industrial applicability. Outside of a moving or stretched cylinder, boundary layer heat transfer viscous flow properties are an important concern in extrusion operations. These investigations have a number of technical applications, including fibre manufacturing and hot rolling. The industrial and technical possibilities of flow over a stretching cylinder have captivated several researchers. Carne [1] described the flow via a stretched plate. Lin and Shih [2,3] glanced at how heat moves through the laminar boundary layer when cylinders move horizontally and vertically with a fixed velocity. Gupta [4] used suction or blowing to achieve mass and heat transfer on a stretched surface. The heat transport parameters of a stretched sheet with changeable temperature were determined by Grubka and Bobba [5]. Minkowycz and Cheng [6] investigated natural convection in a porous material around a vertical cylinder. Malik et al. [7] discussed the impact of viscous dissipation on the MHD heat transmission flow of Sisko fluid through a stretched cylinder. Saeid [8] studied natural convection fluid flow and heat transfer from a horizontal cylinder using a non-equilibrium model. Ali et al. [9] investigated viscous flow through a porous, stretching (shrinking) cylinder. Majeed et al. [10] explored the heat transfer of boundary layer flow across a hyperbolic stretched cylinder. The influence of Hall current on MHD mixed convective flow along a stretched flat vertical plate was studied by Ali et al. [11]. Veera Krishna et al. [12] deliberate the numerical examination of unsteady convective MHD rotating flow over an infinite moving vertical porous surface. Veera Krishna et al. [13] examined Hall and ion slip effects on MHD ciliary propulsion across porous substrates. Veera Krishna and Chamkha [14] deliberated the effect of ion slip and hall current on MHD rotational flow via porous material. Veera Krishna et al. [15] studied radiation absorption on MHD nanofluid convection via a vertically moving absorbent plate.

Heat source/sink has applications in issues involving dissociating fluids, chemical processes, and may affect the rate of particle deposition. In renewable energy and waste heat recovery, heat source/sink chillers are employed. Several absorption methods include a generator-to-air heat exchanger, a compression-to-air heat pump, and a discrete heating system. Abbas et al. [16] discussed the impact of radiation on MHD flow through a stretched cylinder in a porous material. Chauhan et al. [17] used radiation to evaluate MHD and heat transport in a porous media past a stretched cylinder. Chamkha [18] examined the mass and heat transfer associated with MHD fluid flow through a poignant permeable cylinder, including heat production/absorption. Sharma et al. [19] examined the MHD heat transfer fluid flow via a Circular Cylinder that was moderately occupied with non-Darcy Porous Medium. Abel et al. [20] considered the heat transfer characteristics of an upper-convective Maxwell MHD fluid over a stretched surface. The effect of radiation on Jeffery fluid with nanoparticles on a surface of changing thickness under the impact of heat production was explored by Yogesh et al. [21]. Emad et al. [22] explored the pressure drop and thermal performance of a nanofluid in micro heat absorption with a novel circular shape for cooling electronic equipment. Ion and Hall slip impacts on rotating MHD nanofluid flow along an infinite vertical flat plate surrounded by a porous medium were explored by VeeraKrishna and Chamkha [23]. Veera Krishna et al. [24,25] deliberated the impact of heat production/sink on unsteady MHD natural convection second-grade fluid flow revolving along an exponentially accelerating plate. The influence of thermal radiation on MHD dusty fluid through a stretched cylinder entrenched in a porous media in the occurrence of heat generation was investigated by Manjunatha et al. [26]. The effects of magnetic field on heat transfer fluid flow in various geometries are investigated in [27–30].

The current paper focuses on the viscous, steady boundary layer flow of an electrically conducting Newtonian viscous fluid, in the presence of a magnetic field, as well as heat transfer analysis due to a horizontal porous elongating cylinder in the appearance of heat source/sink and a varying surface temperature. Consequently, the purpose of this work is to do such an analysis in the presence of an external magnetic field. It is presumed that the magnetic field is under the strong influence of diffusive effects within the presence of a low magnetic field Reynolds number. Our prime motivation is to extend the study of [32] to incorporate into the transverse magnetic field effects together with the heat source/sink in the corresponding energy equation. It is then intended to work out the effects of these terms, particularly the curvature and heat generation/absorption parameter, on the heat transfer. With the aid of precise similarity transformations, the proposed fluid flow problem's non-linear PDEs are transmuted into a system of ODE's. For this purpose, the current flow problem's nonlinear governing equations are solved numerically using a highly accurate an implicit finite difference approach known as Keller-Box technique. We examined the significant quantities involved in the flow process by drawing their graphs in relation to the parameters of physical significance. For various flow conditions, the skin friction coefficients, and Nusselt number are examined. Industrial and technical applications of the current work include the condensation of a metallic plate in glass, glass fibre manufacturing, polymer industries in a bath, and aerodynamic extrusion of plastic sheets, among others. For the purpose of validating the precision of our numerical calculation, the current findings are compared to previously published data from the existing literature. In addition, no effort has been made to calculate numerical solutions using Keller-Box method for such nonlinear problems in horizontal cylindrical shape. This research consists of five components. Section 1 is special for literature assessment. In phase 2, modelling and system of problems are provided. The third section comprises crucial numerical method procedures. Section four is designated for the discussion of numerical experiment findings. Section five provides an overview of the full examination.

## 2. Formulation:

Consider a steady-state 2-D electrically conducting heat transfer boundary layer Newtonian fluid flow caused by free convection from a horizontal cylinder with radius $a$ and immersed in a porous saturated medium.

The assumptions used to idealize the considered model are stated as follows:

- The cylinder is intended to be overextended in the axial direction with a linear velocity $u_w(x) = U\frac{x}{l}$, and its surface is imperiled to a temperature change $T_w(x) = T_\infty + T_0\left(\frac{x}{l}\right)^n$.
- The $x$-axis is measured parallel to the cylinder's axis, whereas the $r$-axis is radially measured. A homogenous magnetic field of intensity $B$ acting radially.
- Viscous dissipation is omitted in the equation of energy.
- The resultant magnetic field is disregarded in comparison to the applied magnetic field.

The continuity, momentum, and thermal energy equations for this flow are expressed as follows (Ref. [31–34]):

$$\frac{\partial}{\partial x}(ru) + \frac{\partial}{\partial r}(rv) = 0, \quad (1)$$

$$u\frac{\partial u}{\partial x} + v\frac{\partial u}{\partial r} = \frac{v}{r}\frac{\partial}{\partial r}\left(r\frac{\partial u}{\partial r}\right) - \frac{\sigma B^2}{\rho}u - \frac{v}{K_p}u, \quad (2)$$

$$u\frac{\partial T}{\partial x} + v\frac{\partial T}{\partial r} = \frac{\alpha}{r}\frac{\partial}{\partial r}\left(r\frac{\partial T}{\partial r}\right) + \frac{Q_0}{\rho C_p}(T - T_\infty) \quad (3)$$

The boundary criteria are as follows:

$$r = a, u = u_w(x) = U\frac{x}{l}, v = 0, T = T_w(x) = T_\infty + T_0\left(\frac{x}{l}\right)^n$$

$$r \to \infty, T \to T_\infty, u \to 0 \quad (4)$$

The equations (1) – (3) can be reduced to ODE's, by utilizing the following similarity variables:

$$\eta = \frac{r^2 - a^2}{2a}\left(\frac{u_w}{\upsilon x}\right)^{1/2}, \psi = (\upsilon x u_w)^{1/2} a f(\eta), u = \frac{1}{r}\frac{\partial \psi}{\partial r},$$

$$v = -\frac{1}{r}\frac{\partial \psi}{\partial x}, \theta(\eta) = \frac{T - T_\infty}{T_w - T_\infty} \quad (5)$$

With the help of the above transformations, equations (2) and (3) subject to the boundary conditions (4) will take the following form:

$$(1 + 2\eta\beta)f''' - (f\prime)^2 + ff'' + 2\beta f'' - (M + K)f' = 0 \quad (6)$$

$$(1 + 2\eta\beta)\theta'' + 2\delta\theta' + Pr.(f\theta\prime - nf'\theta) + Pr.Q.\theta = 0 \quad (7)$$

The boundary constraints (4) are condensed to.

$$f(0) = 0, f'(0) = 1, \theta(0) = 1, f'(\infty) \to 0, \theta(\infty) \to 0 \quad (8)$$

where prime indicates diff. w.r.to $\eta$.

The surface shearing stress is denoted by.

$$\tau_w = \mu\left(\frac{\partial u}{\partial r}\right)_{r=a} \quad (9)$$

The coefficient of skin friction coefficient $C_f$ is.

$$C_f = \frac{2\tau_w}{\rho u_w^2}$$

$$\Rightarrow \frac{1}{2}C_f Re^{1/2} = f\prime\prime(0), \quad (10)$$

where $Re = \frac{lU}{\upsilon}$ is the Reynolds number.

The heat transfer rate near the sheet is described by $q_w = -\kappa\left(\frac{\partial T}{\partial r}\right)_{r=a}$,

The Nusselt number $Nu_x$ is described as.

$$Nu_x = \frac{xq_w}{\kappa(T_w - T_\infty)}$$

$$\Rightarrow \frac{Nu_x}{Re^{1/2}} = -\theta\prime(0) \quad (11)$$

## 3. Solution of the problem

Eqs. (6) – (7) are nonlinear equations for which closed-form solutions are not attainable; hence, which have been solved numerically by utilizing the Keller-Box approach and captivating into account the boundary constraints quantified in Eq. (8), Keller invented the method, which is commonly considered as very advantageous for solving nonlinear problems and is readily applicable to any particular order. The critical aspects of this strategy for finding approximate solutions are:

i. Change the specified collection of first-order D.E's into a collection of linear equations.

ii. Convert the modified ODEs to finite differences.
iii. Newton's approach is utilized to linearize the algebraic equations and convert them to vector matrix-form.
iv. Subsequently, the collection of linear equations is solved by means of the block tri-diagonal elimination approach.

The present technique is unconditionally reliable, consistent, and straightforward to program, which results in an exceedingly desired outcome. The adaptation of the associated initial estimate is one of the elements that affect the scheme's consistency. Consistency in treatment is contingent upon making the correct choice. On the basis of convergence criteria and compliance with the boundary restrictions (8), the following initial expectations are considered:

$$f(\eta) = 1 - e^{-\eta}, \theta(\eta) = e^{-\eta} \quad (12)$$

The present study used a uniform grid size of $\Delta\eta = 0.005$, which gives 4 decimal places of precision for most of the provided values in the table, with an error tolerance $10^{-5}$ in every instance.

## 4. Results and discussion

The Keller-Box strategy is used to solve the collection of non-linear ODE's (6) & (7), as well as the boundary constraints (8), using MATLAB software. To get a better understanding of the fluid flow's behavior, a computational study of the dimensionless velocity and heat transfer profiles over the boundary layer was performed, and the findings are displayed in Figs. 1–9. To illustrate the validity and precision of the current method, a comparison is made between the current numerical findings and previously acquired outcomes, and a high degree of concordance is found.

The influence of increasing the magnetic field intensity on the thickness of the momentum boundary layer is demonstrated in Fig. 1. It is now well documented that the magnetic field dampens the velocity by generating drag force that opposes the motion of the fluid, resulting in a decrease in velocity. The magnetic field resists transport phenomena. This is because a change in $M$ causes a change in the Lorentz force owing to the magnetic field, and the Lorentz force generates

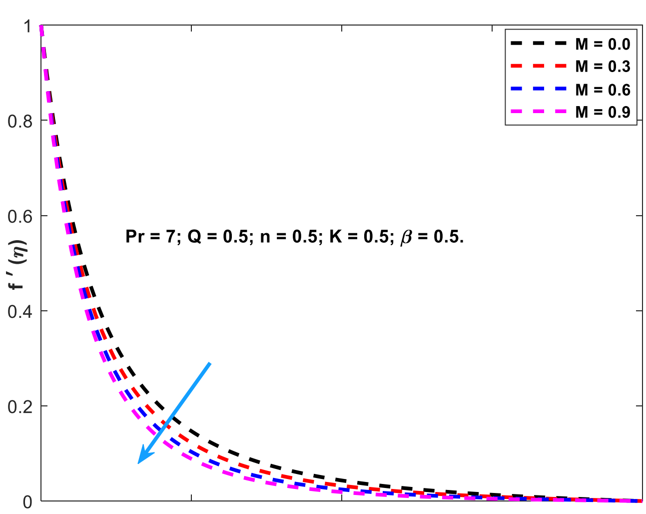


**Fig. 1** Velocity Profile vs Magnetic parameter.

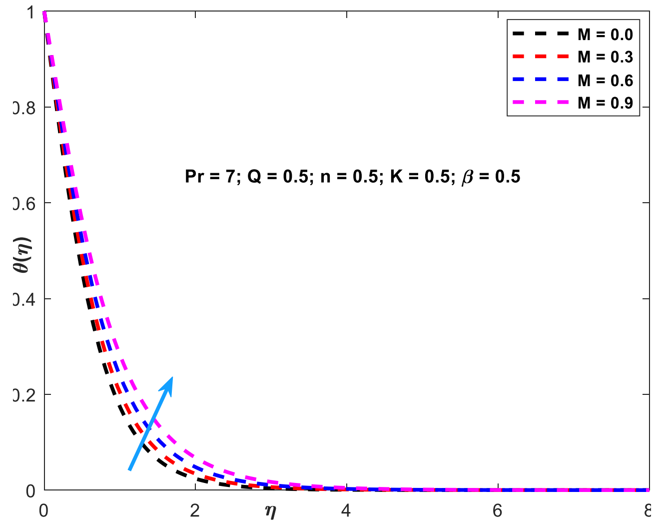


**Fig. 2** Temperature Profile vs Magnetic parameter.

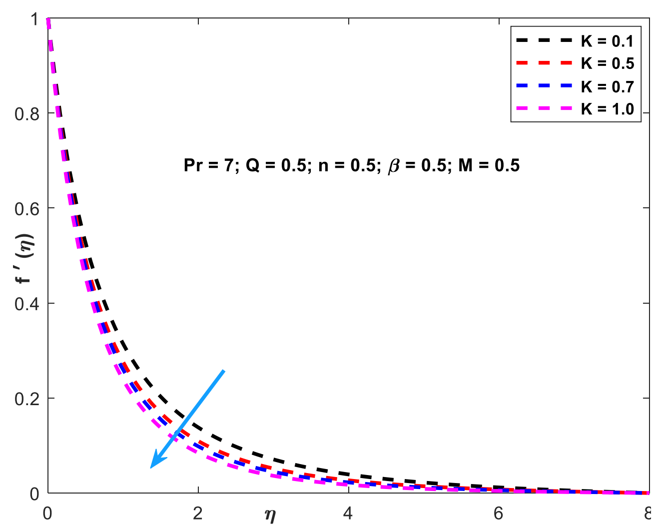


**Fig. 3** Velocity Profile vs Permeability parameter.

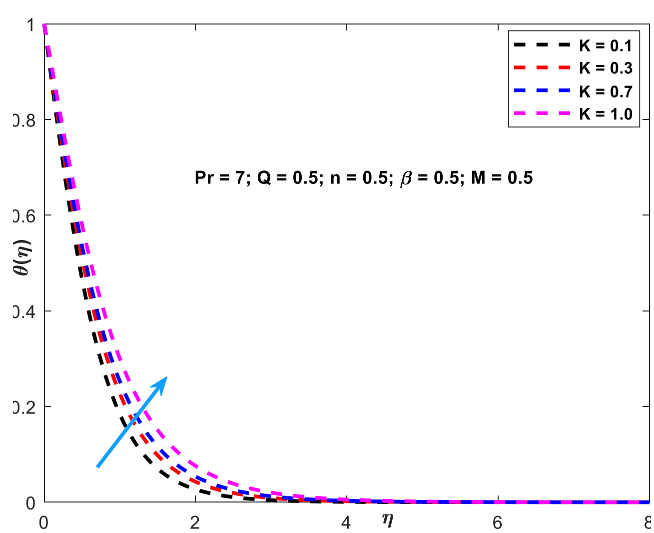


**Fig. 4** Temperature Profile vs Permeability parameter.

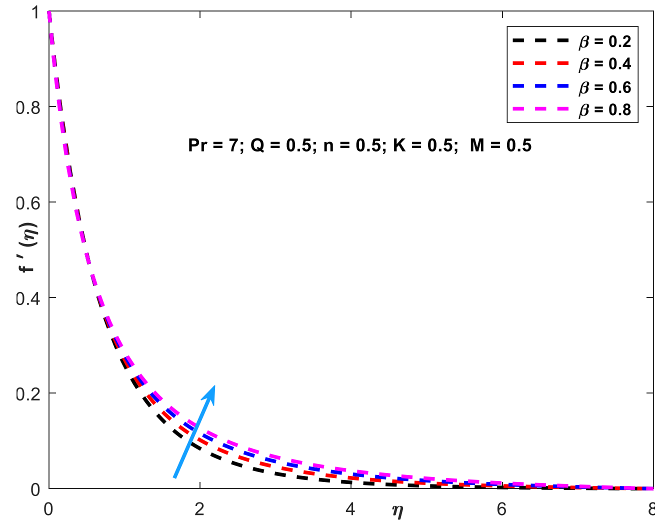


**Fig. 5** Velocity Profile vs Curvature parameter.

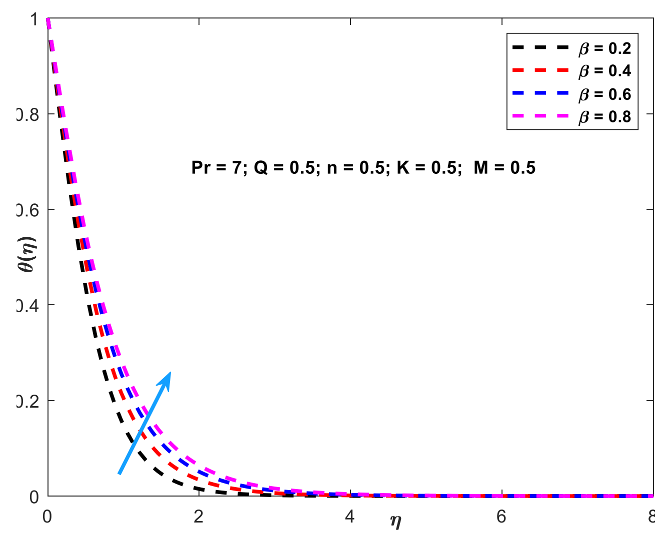


**Fig. 6** Temperature Profile vs Curvature parameter.

more resistance to transport events. In all circumstances, velocity vanishes at a considerable distance from the tube's surface. Fig. 2 illustrates the influence of the magnetic parameter (M) on the temperature. When seen in Fig. 2, the thickness of the thermal boundary layer grows as the magnetic parameter is increased.

The effects of the porosity factor on velocity and fluid temperature gradients are depicted in Figs. 3 and 4. It is obvious that the existence of a porous media results in increased fluid flow restriction, instigating it to move more and more slowly, which therefore decreases the fluid's velocity. Consequently, the impedance to fluid motion rises as the permeability factor enhances. Subsequently, the boundary layer temperature increases as a result of a reduction in fluid velocity. Thus, it can be argued that a rise in $K$ reduces the thickness of the boundary layer, resulting in a rise in the rate of heat transfer. The effect of curvature parameter on velocity and temperature profiles is seen in Figs. 5 and 6. As the curvature parameter is increased, it is noticed that both the profiles are enhanced. This

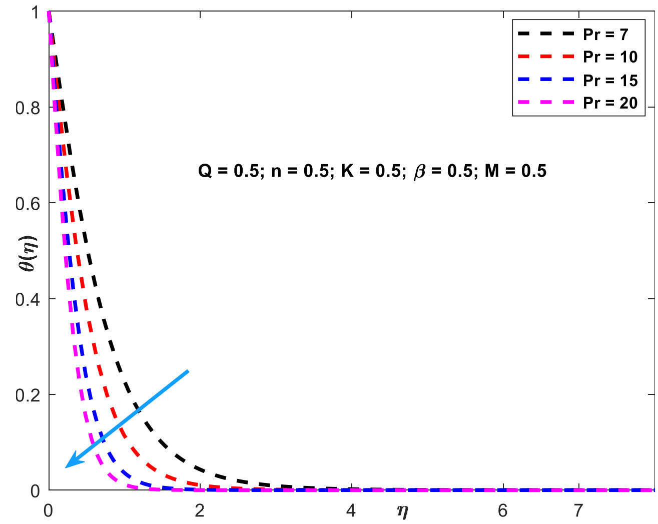


**Fig. 7** Temperature Profile vs Prandtl number.

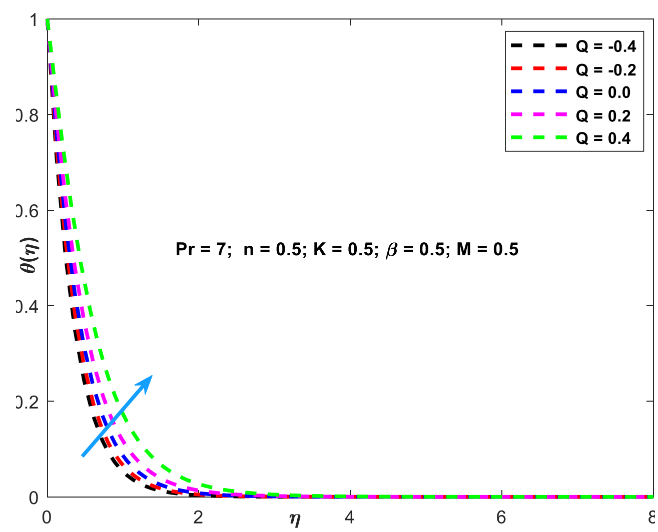


**Fig. 8** Temperature Profile vs Heat source/sink parameter.

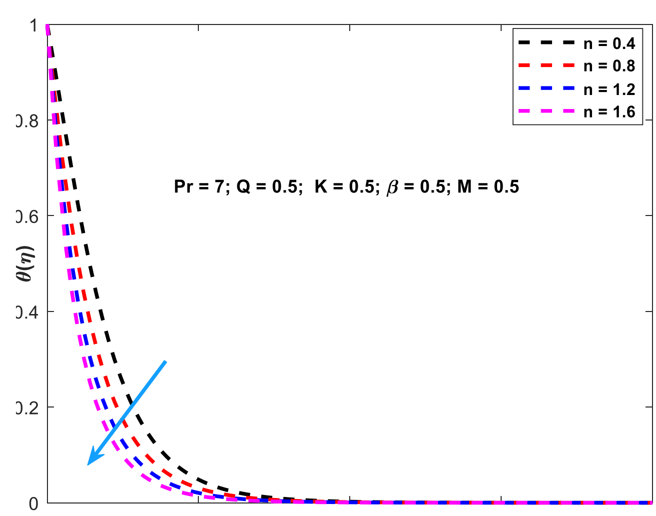


**Fig. 9** Temperature distribution vs surface temperature exponent.

**Table 1** Comparison of $-f''(0)$ for various values of $M$ *when* $K = 0$ and $\beta = 0$.

| M | Abel et al [20] | Yadav & Sharma [32] | Present Results |
|---|---|---|---|
| 0 | −0.999962 | −0.999962 | −0.9999498 |
| 0.2 | −1.095445 | −1.095445 | −1.09544512 |

is clear from practical observation, since fluid flows significantly quicker over a cylinder with a small radius than over a cylinder with a vast radius or a flat surface. Because curvature and radius have an inverse connection, increasing curvature leads to a decrease in cylinder surface. The decrease in the surface area improves fluid flow across the surface, increasing velocity and temperature.

The influence of Prandtl number $Pr$ on the temperature field is inspected in Fig. 7. Increases in $Pr$ result in a diminution in the thermal boundary layer, which outcomes in a decrease in the temperature profile. When the Prandtl number is increased, the kinematic viscosity becomes greater than the density, generating a resistive force against the flow of the fluid. Fig. 8 illustrates the impact of the heat source and sink (Q) on the temperature. It is obvious that when the heat production parameter is increased, the temperature profiles become more pronounced. The heat source factor reflects the production of heat that is dispersed all over when $Q$ is positive, $Q$ is negative, the heat absorption, and $Q = 0$ there is no heat source. It can be detected that the boundary thermal layer creates energy, which causes the temperature of the fluid to grow as the value of $(Q > 0)$ increases, whilst the temperature is lowest for $(Q < 0)$.

When seen in Fig. 9, as the exponent of the surface temperature $(n)$ grows, the temperature profiles decrease. This shows that the velocity field slowed down by growing the temperature exponent quantities.

To confirm the approach employed in this work and to assess its correctness, the computational approximated quantities of the friction factor and local Nusselt number for the

**Table 2** Comparison of $-\theta\prime(0)$ for different values of Pr and $n$ with $Q = M = \beta = K = 0$.

| Pr | $n$ | Grubka [5] | F.M. Ali et al. [11] | Abel et al. [20] | Yadav & Sharma [32] | Present study |
|---|---|---|---|---|---|---|
| 0.72 | 1 | 0.8086 | 0.8086 | – | 0.808689 | 0.80868054 |
| 1 | 1 | 1 | 1 | 1.000174 | 1 | 1.00000117 |
| 3 | −1 | 0 | – | – | −0.03872 | 0.00000137 |
| 3 | 0 | 1.1652 | – | – | 1.154551 | 1.16525326 |
| 3 | 1 | 1.9237 | 1.9237 | 1.923609 | 1.9237 | 1.92367744 |
| 3 | 2 | 2.5097 | – | – | 2.515901 | 2.5097091 |
| 10 | −1 | 0 | – | – | −0.08075 | −0.25924948 |
| 10 | 0 | 2.308 | – | – | 2.299989 | 2.30801969 |
| 10 | 1 | 3.7207 | 3.7208 | – | 3.719976 | 3.72059137 |
| 10 | 2 | 4.7969 | – | – | 4.808102 | 4.79674206 |

**Table 3** Numerical computations of friction factor $-f\prime\prime(0)$ and Nusselt $-\theta\prime(0)$ number for several quantities of physical factors.

| | | | | | | Yadav & Sharma [32] | | Present study | |
|---|---|---|---|---|---|---|---|---|---|
| $Pr$ | $Q$ | $n$ | $K$ | $M$ | $\beta$ | $-f''(0)$ | $-\theta\prime(0)$ | $-f''(0)$ | $-\theta\prime(0)$ |
| 20 | 0.5 | 0.5 | 0.5 | 0.5 | 0.5 | 1.568286 | 2.146312 | 1.62657 | 2.569709 |
| 50 | 0.5 | 0.5 | 0.5 | 0.5 | 0.5 | 1.568286 | 4.485325 | 1.626569 | 4.649702 |
| 100 | 0.5 | 0.5 | 0.5 | 0.5 | 0.5 | 1.568286 | 6.985691 | 1.626568 | 6.98796 |
| 7 | −0.5 | 0.5 | 0.5 | 0.5 | 0.5 | 1.568286 | 3.227012 | 1.626586 | 2.857171 |
| 7 | 0 | 0.5 | 0.5 | 0.5 | 0.5 | 1.568286 | 2.523121 | 1.626588 | 2.181592 |
| 7 | 0.5 | 0.5 | 0.5 | 0.5 | 0.5 | 1.568286 | 1.023121 | 1.626571 | 1.096769 |
| 7 | 0.5 | 1 | 0.5 | 0.5 | 0.5 | 1.568286 | 1.823197 | 1.626572 | 1.901911 |
| 7 | 0.5 | 1.5 | 0.5 | 0.5 | 0.5 | 1.568286 | 2.703146 | 1.626572 | 2.522447 |
| 7 | 0.5 | 0.5 | 1 | 0.5 | 0.5 | 1.741353 | 1.20376 | 1.799333 | 0.900114 |
| 7 | 0.5 | 0.5 | 1.5 | 0.5 | 0.5 | 1.896457 | 1.137402 | 1.954197 | 0.564435 |
| 7 | 0.5 | 0.5 | 2 | 0.5 | 0.5 | 2.038344 | 0.80074 | 2.09585 | −0.84079 |
| 7 | 0.5 | 0.5 | 0.5 | 0 | 0.5 | 1.368981 | 1.168357 | 1.427481 | 1.253101 |
| 7 | 0.5 | 0.5 | 0.5 | 0.3 | 0.5 | 1.492376 | 1.17074 | 1.550774 | 1.161786 |
| 7 | 0.5 | 0.5 | 0.5 | 0.7 | 0.5 | 1.640082 | 1.185342 | 1.698245 | 1.025802 |
| 7 | 0.5 | 0.5 | 0.5 | 0.5 | 0.3 | 1.509707 | 1.003791 | 1.544245 | 1.211402 |
| 7 | 0.5 | 0.5 | 0.5 | 0.5 | 0.7 | 1.623808 | 1.064235 | 1.706244 | 1.02508 |
| 7 | 0.5 | 0.5 | 0.5 | 0.5 | 1 | 1.702086 | 1.104235 | 1.821814 | 0.963679 |

stretched cylinder are numerically compared to those reported by Gurbka [5], F.M. Ali et al. [11], Abel et al. [20] and Yadav & Sharma [32]. There is a high degree of consistency between the findings in Table 1, and Table 2, it instills trust in the numeric data presented later. Table 3 displays the fluctuation of the reduced Nusselt number and skin-friction coefficient with regard to $Pr, Q, M, n, K\&\beta$. As the increasing values of $K, M$, and $\beta$ the local Nusselt number $-\theta\prime(0)$ falls, nevertheless, skin-friction coefficient $-f\prime\prime(0)$ rises. The rate of heat transmission increases as the amounts of $Pr$ and $n$ accumulate, whereas the reverse tendency is seen for the heat generation/absorption parameter $Q$.

## 5. Concluding remarks

The numerical study is accomplished on the impact of MHD heat transfer boundary layer flow of an incompressible viscous fluid over a continuously expanding horizontal cylinder immersed in a porous material in the occurrence of heat source or sink. By employing similarity variables, the PDE's are changed to ODE's. The Keller-Box scheme is used to attain the desired results. The diagrammatic representation of the effect of several important flow parameters on velocity and temperature profiles are discussed. The numerical findings were found to be in great accordance with the outcomes of Yadav et al. [32]. The research focuses primarily on the influence of the curvature parameter of the stretching cylinder, which is a crucial element influencing both fluid velocity and temperature factors. In addition, the impacts of the applied magnetic field, the temperature-dependent heat production/absorption factor, and the Prandtl number are considered. The following are critical observations:

- The parameters $M$ & $K$ upsurges, the flow which consequences in a diminution in velocity profile and enhances the thermal gradient.
- The thickness of the thermal boundary layer upsurge with an escalation of the factors $\beta$ & $Q$.
- With an increase of $\beta$, the results in velocity enhancement.
- With the increase of $Pr$ & $n$, there is a decrement in the temperature profiles.
- The skin friction coefficient rises as the magnetic field parameter $(M)$, Porosity factor $(K)$, and curvature parameter $(\beta)$ rise, but the Nusselt number exhibits the opposite pattern.

## Declaration of Competing Interest

The authors declare that they have no known competing financial interests or personal relationships that could have appeared to influence the work reported in this paper.

## Acknowledgments

The authors extend their appreciation to the Deanship of Scientific Research at King Khalid University for funding this project under grant number (R.G.P. 2/85/43).

## References

[1] L.J. Carne, Flow past a stretching plate, Z. Angew. Math. Phys. 21 (1970) 645–647.
[2] H.T. Lin, Y.P. Shih, Laminar boundary layer heat transfer along static and moving cylinders, J. Chin. Inst. Eng. 3 (1980) 73–79.
[3] H.T. Lin, Y.P. Shih, Buoyancy effects on the laminar boundary layer heat transfer along vertically moving cylinders, J. Chin. Inst. Eng. 4 (1981) 47–51.
[4] P.S. Gupta, Heat and mass transfer on a stretching sheet with suction or blowing, Can. J. Chem. Eng. 55 (1977) 744–746.
[5] L.J. Grubka, K.M. Bobba, Heat transfer characteristics of a continuous stretching surface with variable temperature, J. Heat Transfer 107 (1985) 248–250.
[6] W.J. Minkowycz, P. Cheng, Free convection about a vertical cylinder embedded in a porous medium, Int. J. Heat Mass Transfer 19 (1976) 805–813.
[7] M.Y. Malik, Arif Hussain, T. Salahuddin, M. Awais, Effects of viscous dissipation on MHD boundary layer flow of Sisko fluid over a stretching cylinder, AIP Advances 6 (2016) 035009, https://doi.org/10.1063/1.4944347.
[8] N.H. Saeid, Analysis of free convection about a horizontal cylinder in a porous media using a thermal non-equilibrium model, Int. Commu. Heat Mass Trans. 33 (2006) 158–165.
[9] A. Ali, D.N.K. Marwat, S. Asghar, Viscous flow over a stretching (shrinking) and porous cylinder of non-uniform radius, Adv. Mech. Eng. 11 (9) (2019) 1–9, https://doi.org/10.1177/1687814019879842.
[10] A. Majeed, T. Javed, I. Mustafa, Heat transfer analysis of boundary layer flow over hyperbolic stretching cylinder, Alex. Eng. J. 55 (2016) 1333–1339.
[11] F.M. Ali, R. Nazar, N.M. Arifin, I. Pop, Effect of Hall current on MHD mixed convection boundary layer flow over a stretched vertical flat plate, Meccanica 46 (2011) 1103–1112.
[12] M. Veera Krishna, N. Ameer Ahamad, A.J. Chamkha, Numerical investigation on unsteady MHD convective rotating flow past an infinite vertical moving porous surface, Ain Shams Eng. J. 12 (2) (2021) 2099–2109.
[13] M. Veera Krishna, C.S. Sravanthi, R.S.R. Gorla, Hall and ion slip effects on MHD rotating flow of ciliary propulsion of microscopic organism through porous media, Int. Commun. Heat Mass Transfer 112 (2020) 104500.
[14] M. Veera Krishna, A.J. Chamkha, Hall and ion slip effects on MHD rotating flow of elastico-viscous fluid through porous medium, Int. Commun. Heat Mass Transfer 113 (2020) 104494.
[15] M. Veera Krishna, N. Ameer Ahamad, A.J. Chamkha, Radiation absorption on MHD convective flow of nanofluids through vertically travelling absorbent plate, Ain Shams Eng. J. 12 (3) (2021) 3043–3056.
[16] Z. Abbas, A. Majeed, T. Javed, Thermal radiation effects on MHD flow over a stretching cylinder in a porous medium, Heat Transf. Res. 44 (8) (2013) 703–718.
[17] D.S. Chauhan, P. Rastogi, R. Agrawal, Magnetohydrodynamic flow and heat transfer in a porous medium along a stretching cylinder with radiation, Homotopy Analysis Method. Afrika Matematika 25 (1) (2014) 115–134.
[18] Chamkha AJ. Heat and mass transfer from MHD flow over a moving permeable cylinder with heat generation or absorption and chemical reaction. Communications in Numerical Analysis 2011(2011):20. doi 10.5899/2011/cna-00109.
[19] M.K. Sharma, Kuldip Singh, Ashok Kumar MHD flow and heat transfer through a circular cylinder partially filled with non-darcy porous media, Int. J. Innovat. Technol. Explor. Eng. 4(7) (2014) 30–42.

[20] M.S. Abel, J.N. Tawade, M.M. Nandeppanavar, MHD flow and heat transfer for the upper-convected Maxwell fluid over a stretching sheet, Meccanica 47 (2012) 385–393.

[21] Yogesh Dadhich, Reema Jain, Abdul Razak Kaladgi, Mamdooh Alwetaishi, Asif Afzal, C. Ahamed Saleel, Thermally radiated Jeffery fluid flow with nanoparticles over a surface of varying thickness in the influence of heat source, Case Stud. Therm. Eng. 2021;28:101549.

[22] E.E. Mahmoud, E.A. Algehyne, M.M. Alqarni, A. Afzal, M. Ibrahim, Investigating the thermal efficiency and pressure drop of a nanofluid within a micro heat sink with a new circular design used to cool electronic equipment, Chem. Eng. Commun. (2021) 1035–1047, https://doi.org/10.1080/00986445.2021.1935254.

[23] M. Veera Krishna, A.J. Chamkha, Hall and ion slip effects on MHD rotating boundary layer flow of nanofluid past an infinite vertical plate embedded in a porous medium, Resul. Eng. 15 (2019) 102652.

[24] M. Veera Krishna, N. Ameer Ahamad, A.J. Chamkha, Hall and ion slip effects on unsteady MHD free convective rotating flow through a saturated porous medium over an exponential accelerated plate, Alex. Eng. J. 59 (2020) 565–577.

[25] M. Veera Krishna, N. Ameer Ahamad, A.J. Chamkha, Hall and ion slip impacts on unsteady MHD convective rotating flow of heat generating/absorbing second grade fluid, Alex. Eng. J. 60 (1) (2021) 845–858.

[26] P.T. Manjunatha, B.J. Gireesha, B.C. Prasannakumara, Effect of radiation on flow and heat transfer of MHD dusty fluid over a stretching cylinder embedded in a porous medium in presence of heat source, Int. J. Appl. Comput. Math DOI 10.1007/s40819-015-0107-x.

[27] S. Jain, S. Bhora, Entropy Generation on MHD slip flow over a stretching cylinder with heat generation/absorption, Int. J. Appl. Mech. Eng. 23 (2) (2018) 413–428, https://doi.org/10.2478/ijame-2018-0024.

[28] M. Veera Krishna, Hall and ion slip effects on radiative MHD rotating flow of Jeffreys fluid past an infinite vertical flat porous surface with ramped wall velocity and temperature, Int. Commun. Heat Mass Transfer 126 (2021) 105399.

[29] M. Veera Krishna, Radiation-absorption, chemical reaction, Hall and ion slip impacts on magnetohydrodynamic free convective flow over semi-infinite moving absorbent surface, Chinese J. Chem. Eng. 34 (2021) 40–52.

[30] M. Veera Krishna, A.J. Chamkha, Hall and ion slip effects on magnetohydrodynamic convective rotating flow of Jeffreys fluid over an impulsively moving vertical plate embedded in a saturated porous medium with Ramped wall temperature, Num. Methods Partial Diff. Equat. 37 (3) (2021) 2150–2177.

[31] A. Ishak, R. Nazar, I. Pop, Magnetohydrodynamic (MHD) flow and heat transfer due to a stretching cylinder, Energy Convers. Manage. 49 (2008) 3265–3269.

[32] R.S. Yadav, P.R. Sharma, Effects of porous medium on MHD fluid flow along a stretching cylinder, Ann. Pure Appl. Math. 6 (1) (2014) 104–113.

[33] C.Y. Wang, Fluid flow due to a stretching cylinder, Phys Fluids 31 (1988) 466–468.

[34] P. Ganesan, P. Loganathan, Magnetic field effect on a moving vertical cylinder with constant heat flux, Heat Mass Transfer 39 (2003) 381–386.